Inducible Nitric Oxide Synthase and Arginase Expression in Heart Tissue during Acute *Trypanosoma cruzi* Infection in Mice: Arginase I Is Expressed in Infiltrating CD68$^+$ Macrophages

Henar Cuervo,[1] Miguel A. Pineda,[1] M. Pilar Aoki,[2] Susana Gea,[2] Manuel Fresno,[1,a] and Núria Gironès[1]

[1]Centro de Biología Molecular Severo Ochoa, Consejo Superior de Investigaciones Cientificas (CSIC)–Universidad Autónoma de Madrid (UAM), Cantoblanco, Madrid, Spain; [2]Departamento de Bioquímica Clínica, Centro de Investigaciones en Bioquímica Clínica e Immunologia (CIBICI)–Consejo Nacional de Investigaciones Cientificas y Técnicas (CONICET), Facultad de Ciencias Químicas, Universidad Nacional de Córdoba, Argentina

In Chagas disease, which is caused by *Trypanosoma cruzi,* macrophages and cardiomyocytes are the main targets of infection. Classical activation of macrophages during infection is protective, whereas alternative activation of macrophages is involved in the survival of host cells and parasites. We studied the expression of inducible nitric oxide synthase (iNOS) and arginase as markers of classical and alternative activation, respectively, in heart tissue during in vivo infection of BALB/c and C57BL/6 mice. We found that expression of arginase I and II, as well as that of ornithine decarboxylase, was much higher in BALB/c mice than in C57BL/6 mice and that it was associated with the parasite burden in heart tissue. iNOS and arginase II were expressed by cardiomyocytes. Interestingly, heart-infiltrated CD68$^+$ macrophages were the major cell type expressing arginase I. T helper (Th) 1 and Th2 cytokines were expressed in heart tissue in both infected mouse strains; however, at the peak of parasite infection, the balance between Th1 and Th2 predominantly favored Th1 in C57BL/6 mice and Th2 in BALB/c mice. The results of the present study suggest that Th2 cytokines induce arginase expression, which may influence host and parasite cell survival but which might also down-regulate the counterproductive effects triggered by iNOS in the heart during infection.

Trypanosoma cruzi, a flagellated protozoan parasite, is the causative agent of Chagas disease, an illness that affects several million people in Latin America. During *T. cruzi* infection, macrophages are one of the most important cell types to fight the parasite. These cells metabolize L-arginine via 2 main pathways. The first pathway involves inducible nitric oxide synthase (iNOS), which is responsible for nitric oxide (NO) production. This pathway is controlled by T helper (Th) 1 cytokines known to induce expression of iNOS and by classical activation of macrophages (M1), and it is essential for the early control of infection in mice [1], macrophages [2, 3], and cardiomyocytes [4]. However, excessive amounts of NO can also produce a cytotoxic effect in the host and can lead to immune suppression of T cells [5] and to pathological findings [6].

The second pathway involves arginase, which is induced during alternative activation of macrophages (M2), mainly by Th2 cytokines [7]. Arginase catalyzes conversion of L-arginine to urea and L-ornithine, which is required for polyamine synthesis, which is, in turn, essential for the growth of cells and all trypanosomatidae. The limiting enzyme in this pathway is ornithine

Received 12 July 2007; accepted 6 November 2007; electronically published 12 May 2009.

Potential conflict of interest: none reported.

Presented in part: 16th European Congress of Immunology, 6–9 September 2006, Paris, France (abstract PA-3105).

Financial support: "Ministerio of Ciencia y Tecnología" (grants SAF 2004-0510 and SAF2005-02220); "Fondo de Investigaciones Sanitarias" (grant PI060388); "Red Temática de Investigación en Enfermedades cardiovasculares" (network grant C03/01); "Red de Investigación de Centros de Enfermedades Tropicales" (network grant RD06/0021/0016); "Consejo Superior de Investigaciones Cientificas"–Consejo Nacional de Investigaciones Cientificas y Técnicas and Banco de Santander Central Hispano–Universidad Autónoma de Madrid Spanish Argentinean Collaborative projects; "Comunidad de Madrid" and "Fundación Ramón Areces."

[a] Both authors contributed equally to the direction of this work.

Reprints or correspondence: Dr. Núria Gironès, Centro de Biología Molecular Severo Ochoa, CSIC-UAM, Departamento de Bioquímica y Biología Molecular, Facultad de Ciencias, Universidad Autónoma de Madrid, Cantoblanco, 28049 Madrid, Spain (ngirones@cbm.uam.es).

The Journal of Infectious Diseases 2008; 197:1772–82

0022-1899/2008/19712-0019$15.00
DOI: 10.1086/529527

decarboxylase (ODC), which has a short half-life [8]. Two arginase isoforms have been described. Arginase I, which is located in the cytoplasm, has restricted expression and is mainly induced by Th2 cytokines but, also, by interleukin (IL)–10 [9] and transforming growth factor (TGF)–β [10]. Arginase II, which is located in the mitochondria, is induced in many cell types by lipopolysaccharide (LPS) and cyclic adenosine monophosphate [11]. *N*-hydroxy-L-arginine, an intermediary in NO synthesis, inhibits arginase [12], whereas polyamines can reduce iNOS expression [13, 14]. Moreover, arginase has been implicated in the down-regulation of iNOS protein synthesis and stability by decreasing L-arginine availability [15, 16], which is dependent on cationic amino acid transporter (CAT)–1 and CAT-2 [17, 18].

Helicobacter pylori [19, 20] and *Chlamydia* species [21] can modulate the aforementioned metabolic routes. The balance between arginase and iNOS also modifies the outcome of several protozoan infections. Induction of macrophage arginase during *Trypanosoma brucei* infection depletes L-arginine and may avoid NO-dependent parasite killing [22]. Moreover, arginase and alternative activation play a crucial role in the development of chronic infection with *Trypanosoma congolense* [23]. During in vitro infection with *Leishmania* species [24, 25], as well as during in vivo infection with *Leishmania major* [26, 27], arginase inhibitors reduce the number of pathological findings observed by lowering parasite replication.

On the other hand, in infected cardiomyocytes [4] and macrophages [28], *T. cruzi* triggers the synthesis of cytokines and chemokines that induce potent NO-dependent trypanocidal activity [3, 29–31]. However, peripheral blood monocytes showed decreased NO production during *T. cruzi* infection in rats, because of the increase in arginase activity [32]. Cruzipain, a major *T. cruzi* antigen, up-regulates arginase activity in macrophages promoting intracellular growth of the parasite [33–35] and induces arginase II in cardiomyocytes promoting their survival [36].

After consideration of all these previous findings, our aim in the present study was to assess the role of classical and alternative activation pathways during experimental infection with *T. cruzi* in mice with different susceptibilities to the disease. The study focused on the most important organs affected in Chagas disease: the heart.

MATERIALS AND METHODS

Parasites and mice. Y and Tulahuén *T. cruzi* strains were obtained from John David (Harvard Medical School, Boston, Massachusetts). Blood trypomastigotes were maintained in infected mice. Six- to 8-week-old BALB/c and C57BL/6 mice (Harlan; Interfauna Iberica) and iNOS$^{-/-}$ mice (NOS2^{tm1Lau}; The Jackson Laboratories) were maintained under pathogen-free conditions, in compliance with European norms [37]. All experiments were performed in groups of 3–5 mice that either were not infected or were infected with 2×10^3 Y trypomastigotes, except when stated otherwise, by means of intraperitoneal injection.

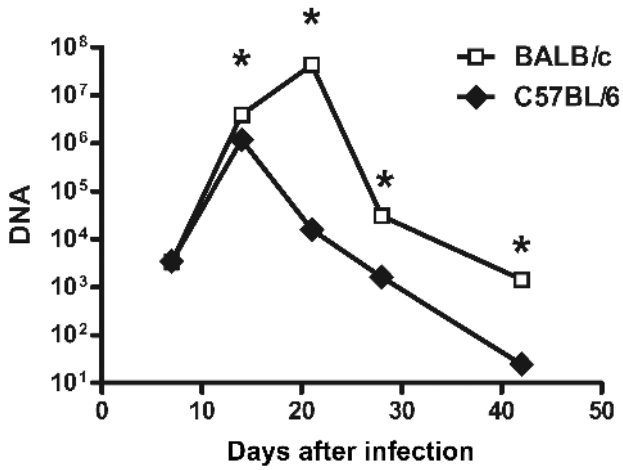

Figure 1. Quantification of *Trypanosoma cruzi* DNA in the heart tissue of infected BALB/c- and C57BL/6 mice. DNA was isolated from heart tissue on the indicated days after infection, and quantitative polymerase chain reaction (PCR) was performed as described in Materials and Methods. *T. cruzi* DNA is expressed as the number of picograms of parasite DNA per milligram of DNA obtained from a heart tissue sample (i.e., picograms of parasite DNA/milligrams of heart tissue). Empty boxes denote values for BALB/c mice, and filled rhombi denote values for C57BL/6 mice. Results are expressed as the mean values (±SD) for triplicates of pooled DNA from 5 different mice. All differences between the parasite loads in BALB/c and C57BL/6 mice were statistically significant, except at 7 days after infection ($P < .05$). A representative experiment (of 3 experiments performed) is shown.

Quantitative real-time polymerase chain reaction (PCR) and reverse-transcription (RT) PCR. Heart DNA was isolated using the High Pure PCR Template Preparation Kit (Roche). Heart tissue samples used in PCR reactions contained 100 ng of genomic DNA, and detection of *T. cruzi* was performed using quantitative real-time PCR, as described elsewhere [38].

RNA was extracted from heart tissue by use of Trizol reagent (Invitrogen). Quantitative real-time RT-PCR analysis was performed using the High Capacity cDNA Archive Kit (Applied Biosystems), and amplification of different genes (arginase I, arginase II, iNOS, CAT-1, CAT-2, ODC, interferon [IFN]–γ, tumor necrosis factor (TNF)–α, interleukin [IL]-4, IL-10, IL-13, TGF-β, prostaglandin E2 synthase (PGE_2S), and ribosomal 18S) was performed in triplicate with the use of TaqMan MGB probes and the TaqMan Universal PCR Master Mix (Applied Biosystems) on an ABI Prism 7900 HT instrument (Applied Biosystems). Quantification of gene expression was calculated using the comparative threshold cycle (C_T) method, normalized to the ribosomal 18S control and efficiency of the RT reaction (relative quantity, $2^{-\Delta\Delta C_T}$).

Protein expression and activity. Heart protein extracts were prepared using a PT 1300 D homogenizer (Polytron). For Western blot analyses, 15 μg of tissue extract was fractionated on

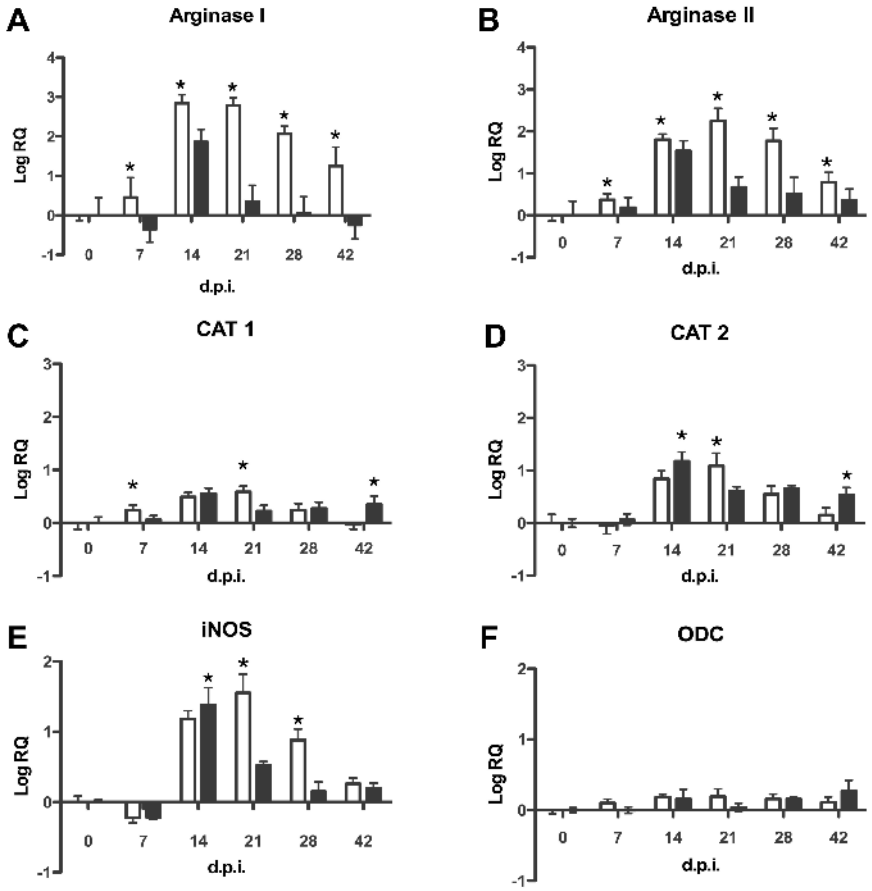

Figure 2. Quantification of enzyme and transporter mRNAs involved in L-arginine metabolism in heart tissue during *Trypanosoma cruzi* infection. RNA from heart tissue was isolated at different days post infection (dpi), and quantitative reverse-transcription polymerase chain reaction was performed. Results are expressed as the logarithm of relative quantity (RQ) calculated from comparative threshold cycle values, as described in Material and Methods. mRNA values for arginase I *(A),* arginase II *(B),* cationic amino acid transporter (CAT)–1 *(C),* CAT-2 *(D),* inducible nitric oxide synthase (iNOS) *(E),* and ornithine decarboxylase (ODC) *(F)* are shown. *Empty bars,* BALB/c mice; *filled bars,* C57BL/6 mice. Results are expressed as mean values (±SD) for 3 different mice. All differences observed between infected mice and noninfected mice were statistically significant, except those for C57BL/6 mice at 7, 21, 28, and 48 dpi *(A);* for C57BL/6 mice at 7 and 48 dpi *(B);* for BALB/c at 42 dpi and for C57BL/6 mice at 7 dpi *(C);* for BALB/c mice at 7 dpi *(D);* for C57BL/6 mice at 7 dpi *(E);* and for BALB/c and C57BL/6 mice at all days after infection *(F).* *Significant differences between BALB/c and C57BL/6 mice ($P < .05$). A representative experiment (of 5 experiments performed) is shown.

SDS–10% polyacrylamide gel and transferred to a nitrocellulose membrane. Primary antibodies were diluted as follows: anti–mouse iNOS (BD Transduction), 1:5000; goat anti–mouse arginase I and actin (Santa Cruz Biotechnology), 1:1000; and anti-ODC (Sigma-Aldrich), 1:100. Membranes were incubated with horseradish peroxidase (HRP) rabbit anti–goat antibody (1:10,000; Sigma-Aldrich) or goat anti–mouse antibody (1:1000; Pierce) as secondary antibody. Proteins were detected using Supersignal reagent (Pierce). Ganglia, spleen, peripheral blood mononuclear (PBMCs), and cultured cells were treated as mentioned above, except for the mechanical disruption. Arginase activity was measured as described elsewhere [39].

Immunohistochemical analysis. The hearts of mice infected with 10^4 Tulahuén trypomastigotes were removed, fixed in 10% neutral buffered paraformaldehyde, and embedded in paraffin. Sections that were 4 μm thick were mounted on gelatin-coated glass slides, deparaffinized, and rehydrated; endogenous peroxidase activity was blocked by incubation with 3% hydrogen peroxide in PBS, permeabilized with 1% Triton X-100 in PBS, and washed; and nonspecific binding was blocked with 2% bovine serum albumin. Samples were incubated with anti–arginase II, anti-iNOS, and isotypic antibodies (Santa Cruz Biotechnology) diluted 1:100; washed with PBS; incubated with anti–rabbit HRP (Sigma-Aldrich) diluted 1:250; incubated with diaminobenzidine and hydrogen peroxide; and counterstained with hematoxylin.

Confocal immunofluorescence. Hearts were fixed in 4% paraformaldehyde in PBS solution, incubated in 30% sucrose solution, embedded in Tissue-Tek O.C.T. compound (Sakura), and frozen. Sections that were 10- to 15-μm thick were fixed in acetone. Incubation with the following antibodies was done at 4°C: 10 μg/mL goat anti–mouse arginase I, rat anti–mouse

CD68 (Serotec), goat IgG (Jackson ImmunoResearch), and rat IgG (BD Transduction) antibodies; $F(ab')_2$ goat anti–rat IgG fluorescein isothiocyanate antibodies (1:50; Serotec); and Cy5-conjugated donkey anti–goat IgG antibodies (1:50; Jackson Immunoresearch). Images were obtained using an LSM510 Meta confocal laser coupled to an Axiovert 200 (Zeiss) microscope.

Cell cultures. BALB/c neonatal cardiomyocyte culture specimens were obtained as described elsewhere [40]. More than 90% of cells were cardiomyocytes, as detected by immunostaining with antibody to muscarinic acetylcholine receptor M2, as described elsewhere [36]. Peritoneal cells were collected by peritoneal lavage with 0.34 mol/L sucrose and were plated in RPMI 1640 with 5% fetal bovine serum; after 4 h, nonadherent cells were removed by washing 3 times with warm PBS, and fresh RPMI 1640 was restored. Trypomastigotes were obtained in cocultures with Vero cells (CCL-81; American Type Culture Collection), and 5 Y trypomastigotes per cardiomyocyte or macrophage were added. Sixteen h later, noninternalized parasites were removed, and cells were cultured in complete RPMI 1640 medium for 48 h. In addition, cardiomyocytes were incubated with IL-4 (20 ng/mL; BioSource International), IFN-γ (25 U/mL; BioSource International), and LPS (1 μg/mL; *Escherichia coli* serotype O26:B6 [Sigma-Aldrich]), as indicated.

Statistical analysis. Data reported for in vivo experiments are the mean values ($\pm$SD) for 3 individual mice. Statistical significance was evaluated using Student's 2-tailed *t* test.

RESULTS

***Expression of L-arginine metabolic enzymes and transporters in the heart tissue of mice infected with* T. cruzi.** BALB/c and C57BL/6 mice were infected, and the number of parasites in heart tissue was quantified by means of quantitative PCR performed on different days post infection (dpi). Figure 1 shows that a maximum parasite load was detected in a C57BL/6 mouse heart at 14 dpi. In contrast, the parasite burden in the heart of BALB/c mice was maximal at 21 dpi and decreased thereafter. Parasite equivalents were significantly higher ($\sim$2 logs above the peak parasite load) in susceptible BALB/c mice than in resistant C57BL/6 mice.

Quantification of arginase I and II mRNAs revealed significantly higher expression in BALB/c mice than in C57BL/6 mice on all days after infection when analysis was performed (figure 2*A* and 2*B*). In contrast, CAT-1, CAT-2, and iNOS mRNA expression was higher in C57BL/6 mice than in BALB/c mice at 14 dpi (figure 2*C*–*E*). However, CAT-1, CAT-2, and iNOS mRNA expression was higher in BALB/c mice at 21 dpi. The induction of ODC mRNA expression was not significantly different from that noted in noninfected controls (figure 2*F*).

Because arginase I mRNA expression showed more marked differences between BALB/c and C57BL/6 mice than did argi-

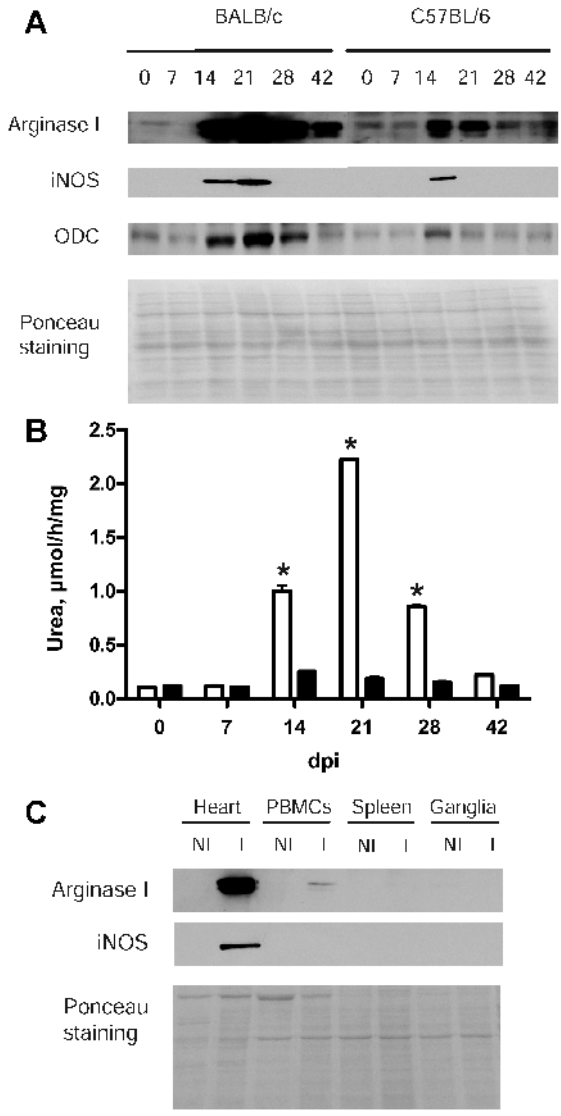

Figure 3. Inducible nitric oxide synthase (iNOS) and arginase I protein expression and activity during *Trypanosoma cruzi* infection in the heart and other tissues. Protein extracts were isolated from heart tissue from 5 BALB/c mice and 5 C57BL/6 mice at different days post infection (dpi) and were pooled for Western blot analysis. *A,* arginase I, iNOS, and ornithine decarboxylase (ODC) expression in and Ponceau staining of the same membrane; numbers denote days after infection. *B,* Arginase activity of the same tissue extracts, expressed as micromoles of urea produced per hour per milligram of protein sample (i.e., μmol/h/mg), was assessed by urea colorimetric determination. *Empty bars,* BALB/c mice; *filled bars,* C57BL/6 mice. All values for BALB/c mice were significantly higher than those for noninfected mice, except at 7 dpi, and those in C57BL/6 were only significantly higher at 14 dpi. *Significant differences between BALB/c and C57BL/6 mice. *C,* Heart tissue, peripheral blood mononuclear cells (PBMCs), spleen, and ganglia were obtained from noninfected (NI) and infected (I) BALB/c mice at 21 dpi. Protein extracts were isolated, and Western blot analyses were performed using anti–arginase I or anti-iNOS antibodies and Ponceau staining. Data are representative of at least 2 independent experiments.

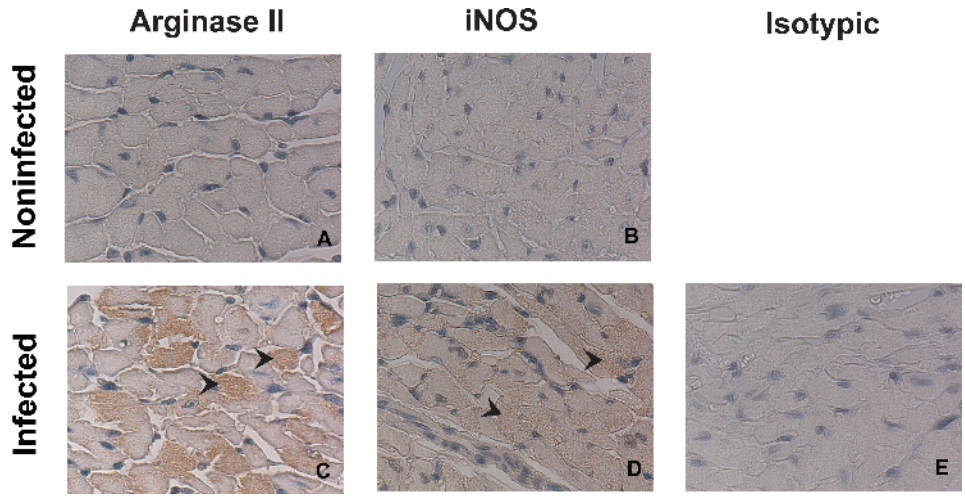

Figure 4. Arginase II and inducible nitric oxide synthase (iNOS) expression by heart tissue from BALB/c mice during acute infection with *Trypanosoma cruzi*. Hearts obtained from noninfected mice and from infected mice at 14 days after infection were analyzed using immunohistochemical analysis, as described in Materials and Methods. Noninfected tissue stained with anti–arginase II antibody *(A)* and with anti–iNOS antibody *(B)*. Infected tissue stained with anti–arginase II antibody *(C)*, with anti–iNOS antibody *(D)*, and isotypic antibody *(E)*. Data are representative of analyses of several sections from ⩾3 different mice. Magnification, ×1000.

nase II expression, we wanted to confirm arginase I findings at the protein level. Induction of arginase I protein in infected heart tissue was much greater in BALB/c mice than in C57BL/6 mice and occurred from 14 to 42 dpi, in agreement with the mRNA data (figure 3*A*). Arginase I expression in C57BL/6 mice was observed only between 14 and 21 dpi. Moreover, arginase enzymatic activity correlated nicely with arginase I protein expression in heart tissue samples from both mice strains (figure 3*B*), being much higher again in BALB/c mice than in C57BL/6 mice, peaking at 21 dpi. In addition, iNOS protein expression was higher in infected BALB/c mice than in infected C57BL/6 mice.

Although we did not observe significant changes in ODC mRNA expression, ODC protein was induced in BALB/c hearts (maximum expression occurred at 21 dpi) and, to a much lower extent, in C57BL/6 mice (peaking at 14 dpi) (figure 3*A*). This indicates that ODC is regulated at the posttranslational level in the heart tissue of mice infected with *T. cruzi*.

We also studied the expression of arginase I and iNOS in the PBMCs, spleen, and ganglia of infected BALB/c mice at 21 dpi. In spleen and ganglia, neither arginase I nor iNOS was induced (figure 3*C*). There was a low expression of arginase I in PBMCs, in comparison with the expression observed in heart tissue, but no iNOS was detected in PBMCs, indicating that arginase I and iNOS are preferentially expressed in heart tissue during acute *T. cruzi* infection.

Expression of arginase II and iNOS by cardiomyocytes and expression of arginase I by CD68⁺ cells infiltrating the heart tissue of* T. cruzi*-infected mice. To determine the cellular source of arginase and iNOS protein detected in the infected hearts, we performed immunohistochemical staining. Figure 4 shows that a high percentage of cardiac fibers stained positive for both arginase II and iNOS in infected BALB/c mice (figure 4*C* and 4*D*), compared with findings in noninfected mice (figure 4*A* and 4*B*).

Arginase I expression in hearts was analyzed by confocal microscopy. Hearts obtained from infected BALB/c mice at 21 dpi showed an infiltrate composed by arginase I–positive cells (figure 5*F*); no staining was observed in cardiomyocytes or endothelial cells. Arginase I–positive infiltrating cells showed a macrophage-like morphology. The CD68 macrophage marker, but not the dendritic cell marker CD11c (data not shown), was found to colocalize with arginase I (figure 5*E–H*) in tissue sections of hearts obtained from *T. cruzi*–infected mice. Noninfected heart tissue showed weak staining with anti-CD68 and anti–arginase I antibodies of some infiltrated resident cells (figure 5*A–D*). No specific staining was observed in sections with isotypic antibodies (figure 5*I* and 5*J*). Next, we evaluated the extension of $CD68^+$ cell infiltration in BALB/c and C57BL/6 mice by quantifying CD68 mRNA. $CD68^+$ cell infiltration was induced at the time of infection and was maximal at 14 dpi in both mouse strains; interestingly, no statistically significant differences were observed between them (figure 5*K*). This similarity in cell infiltration contrasted with observed differences in arginase expression, suggesting that arginase I expression was higher in $CD68^+$ cells from infected BALB/c than in those from infected C57BL/6 mice.

Arginase I expression in primary cultures of cardiomyocytes and macrophages. iNOS and arginase II induction, but no arginase I induction, had been reported during *T. cruzi* infection of cardiomyocytes in vitro [4, 36]. Thus, we infected cardiomyocytes in vitro and analyzed arginase I and iNOS expres-

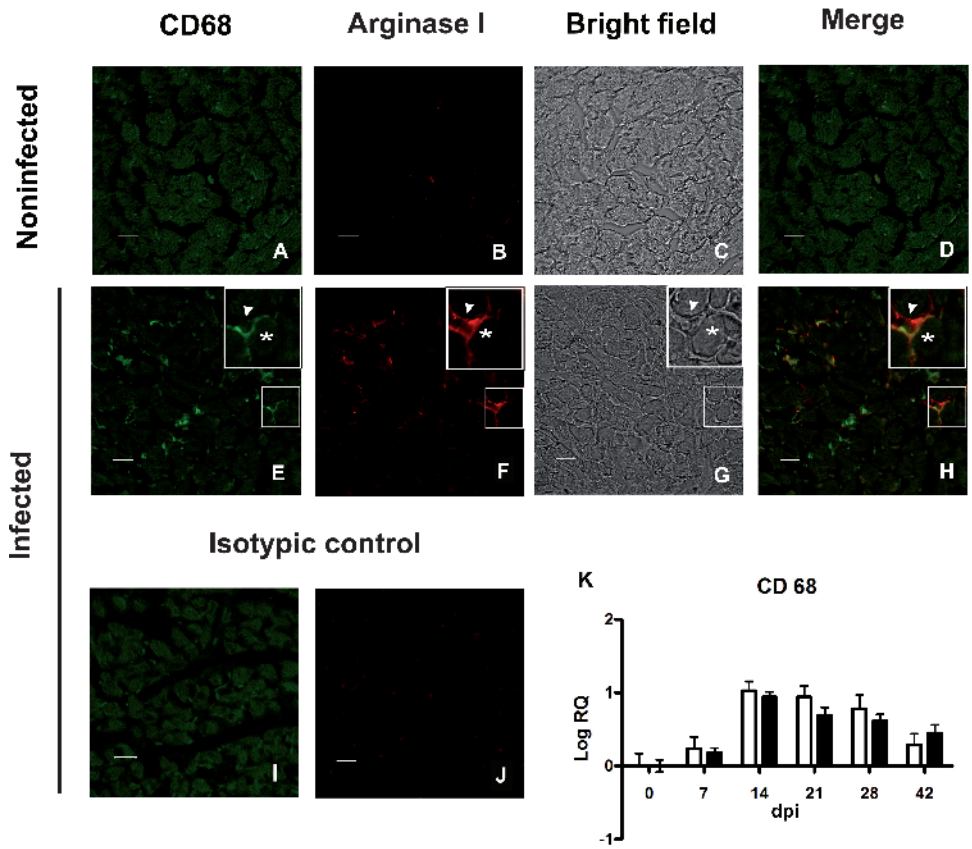

Figure 5. Arginase I and CD68 expression in the heart tissue of BALB/c mice during acute infection with *Trypanosoma cruzi*. Tissue sections obtained from BALB/c mice hearts at 21 days post infection (dpi) were analyzed by immunofluorescence confocal microscopy, as described in Materials and Methods. Noninfected tissue stained with anti-CD68 antibody *(A),* anti–arginase I antibody *(B),* and phase contrast *(C). D,* merge of images *A* and *B.* Infected tissue section stained with anti-CD68 antibody *(E),* anti–arginase I antibody *(F),* and phase contrast *(G). H,* Merge of images *E* and *F (H).* Isotypic control for CD68 antibody *(I)* and arginase I *(J).* Boxed regions are shown at 2-fold magnification of the original magnification (×400) in insets. The scale bar is 20 μm. Data are representative of several sections analyzed in ⩾3 different mice. Total RNA from heart tissue was isolated at 21 days after infection *(K),* and CD68 quantitative reverse-transcriptase polymerase chain reaction was performed as described in Material and Methods. Results are represented as the values mean (±SD) for 3 different mice. All values for BALB/c and C57BL/6 mice were significantly higher than those for noninfected mice. A representative experiment (of 3 experiments performed) is shown. RQ, relative quantity.

sion. iNOS—but no arginase I protein—was induced by infection in cardiomyocytes (figure 6*A*). Besides, the IL-4–dependent arginase I induction in noninfected cardiomyocytes was partially inhibited by *T. cruzi* infection. In contrast, the IFN-γ– and LPS-dependent iNOS induction observed in noninfected cardiomyocytes was strongly potentiated by *T. cruzi* infection of those cells. Therefore, iNOS expression in cardiac cells can be directly triggered by the parasite and is probably responsible for the inhibition of IL-4–dependent arginase I expression (figure 6*A*).

T. cruzi infection triggers NO production in IFN-γ–activated macrophages, but the parasite itself does not induce production of NO in this cell type [28]. We found that in vitro infection of resident peritoneal macrophages in BALB/c mice did not increase arginase I expression (figure 6*B*). Therefore, arginase I induction seen in $CD68^+$ heart-infiltrating cells is not likely triggered by the parasite but, rather, by the inflammatory environment in the heart that is set off during the immunologic response against the parasite.

To test the contribution of the iNOS gene to expression of arginase I in the heart, we infected $iNOS^{-/-}$ mice. The finding that parasitemia in $iNOS^{-/-}$ mice did not significantly change in comparison with that noted in wild-type *(wt)* mice (figure 6*C*) is in agreement with reports published elsewhere [41]. However, the expression (figure 6*D*) and activity (figure 6*E*) of arginase I in the heart were strongly increased in $iNOS^{-/-}$mice, compared with *wt* mice. Thus, deletion of the iNOS gene triggered the increase in the induction of arginase I in the heart tissue of mice infected with *T. cruzi.*

***Induction of both Th1 and Th2 cytokines and PGE_2S in the heart tissue of mice infected with* T. cruzi.** We tested the levels of several cytokines in the heart tissue of mice infected with *T. cruzi,* by means of quantitative mRNA RT-PCR. The results showed that, for IFN-γ and TNF-α, maximum expression oc-

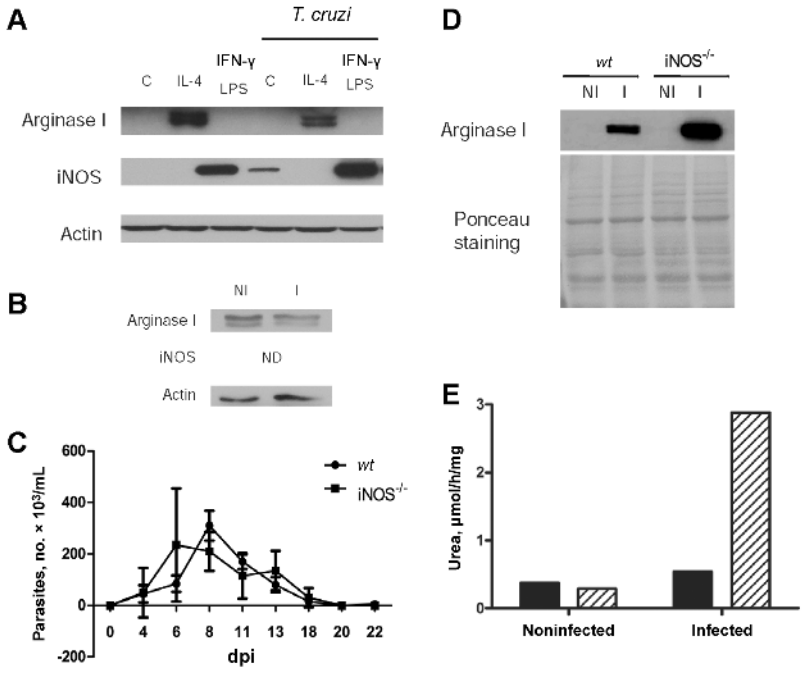

Figure 6. Expression of arginase I and inducible nitric oxide synthase (iNOS) in BALB/c cardiomyocytes, peritoneal macrophages, and heart tissue of iNOS$^{-/-}$ mice. *A,* Western blot analysis of neonatal cardiomyocyte cultures not infected (NI) and infected (I) in vitro with *Trypanosoma cruzi* trypomastigotes cultured with media alone *(C);* interleukin (IL)–4; and lipopolysaccharide and interferon (IFN)–γ, as indicated. Arginase I, iNOS, and actin expression is shown. *B,* Arginase I, iNOS, and actin expression in NI and I macrophage cultures; iNOS expression was not detected (ND). *C,* Parasitemia of infected wild-type *(wt) (filled circles)* and iNOS$^{-/-}$ *(filled squares)* mice. *D,* Arginase I expression of heart tissue extracts pooled from 3 *wt* and 3 iNOS$^{-/-}$ NI and I mice at 21 dpi and Ponceau staining of the same membrane. *E,* Arginase activity of the same extracts expressed as the no. of micromoles of urea produced per hour per milligram of protein sample (i.e., μmol/h/mg). Filled bars denote values for *wt* NI and I mice, and dashed bars denote values for NI and I iNOS$^{-/-}$ mice. Data are representative of at least 2 independent experiments.

curred at 14 and 21 dpi in C57BL/6 and BALB/c mice, respectively (figure 7*A* and *7B*). Expression of these cytokines was significantly higher in C57BL/6 mice than in BALB/c mice at 14 dpi; however, the situation was reversed at 21 dpi and later, when expression was higher in BALB/c mice than in C57BL/6 mice. On the other hand, maximum expression of IL-4 and IL-13 occurred at 14 dpi in both mouse strains, with expression noted to be higher in BALB/c mice than in C57BL/6 mice throughout the period of infection. Interestingly, expression of IL-4 and, especially, IL-13 in BALB/c mice was maintained at 21 dpi (figure 7*C*–7*D*). IL-10 expression in the heart was significantly increased by infection and followed kinetics similar to TNF-α expression (figure 7*E*). The induction of TGF-β mRNA expression that was observed was not statistically different from that noted in noninfected controls (figure 7*F*). PGE_2S mRNA was significantly increased in the hearts of both BALB/c and C57BL/6 mice at the time of infection, being significantly higher in BALB/c mice than in C57BL/6 mice at 21 dpi (figure 7*G*). Thus, no pure Th1 or Th2 patterns are associated with strain susceptibility or infection stage. However, the balance between Th1 and Th2 was higher in C57BL/6 mice (resistant mice) than in BALB/c mice (susceptible mice), and the levels of Th2 cytokine and PGE_2S expression were higher in BALB/c mice than in C57BL/6 mice.

DISCUSSION

Heart leukocyte infiltration is thought to play an important role in the myocarditis associated with *T. cruzi* infection. However, to date, most of the research in the field has focused on characterization of the T cells present in heart inflammatory infiltrate, whereas very little effort has been directed to the study of macrophages. Macrophages may become activated by different pathways, which play different and somehow opposite roles. The results of the present study show, for what we believe is the first time, that arginase expression and activity are strongly induced in heart tissue during acute *T. cruzi* infection in mice, together with increased expression of iNOS. This finding was observed in both susceptible BALB/c mice and resistant C57BL/6 mice. The peak parasite load correlated with peaks in arginase I and iNOS expression in heart tissue. Moreover, arginase I expression in BALB/c mice was higher and persisted for a longer period than it did in C57BL/6 mice, which more efficiently controlled the infection. In addition, ODC protein expression was also induced during the acute phase of infection, suggesting an increase in the polyamine synthesis needed for mammalian cell proliferation but, more importantly, for parasite replication.

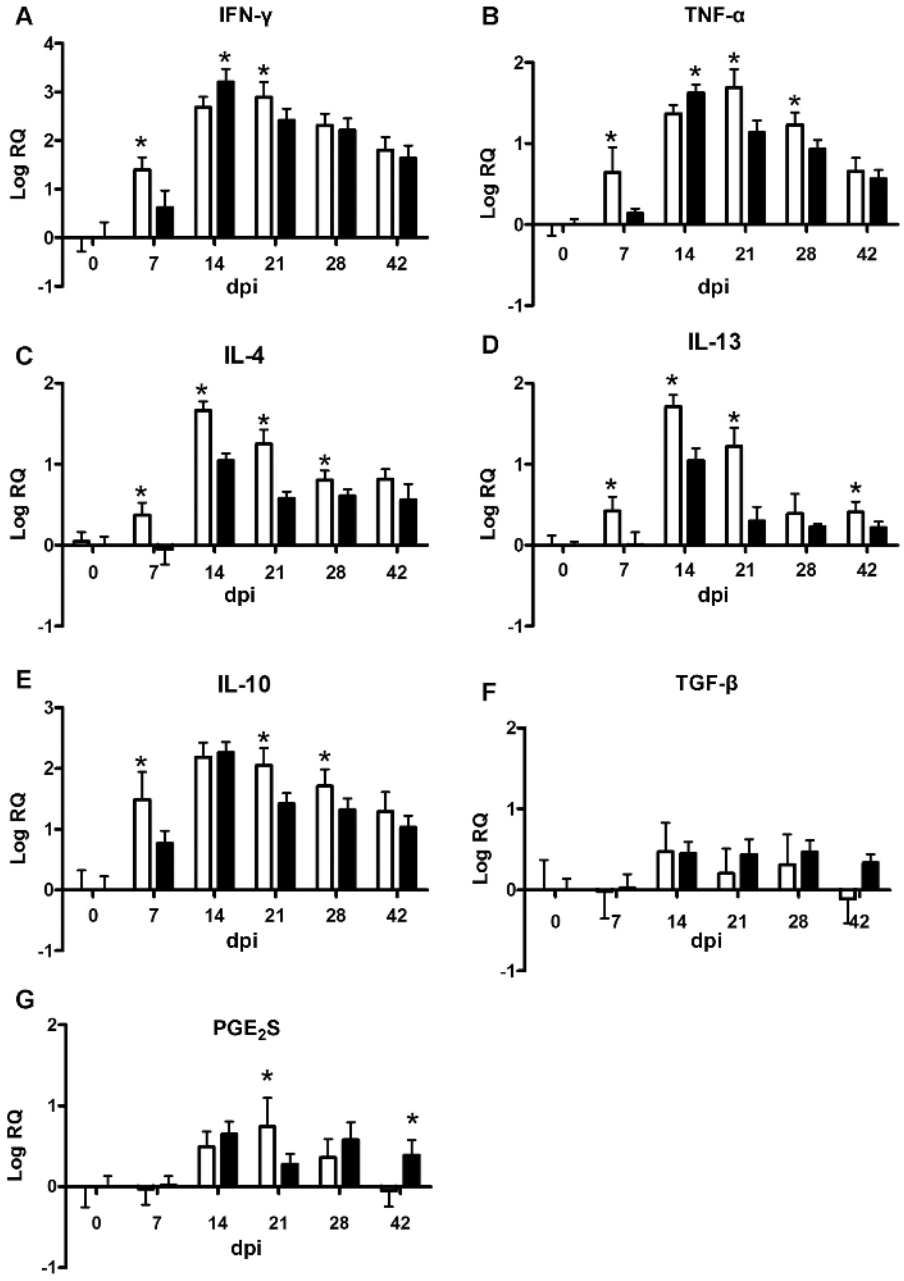

Figure 7. Expression of cytokines and prostaglandin E_2 synthase (PGE_2S) in mouse heart tissue during *Trypanosoma cruzi* infection. Total RNA was isolated in heart tissue obtained from BALB/c and C57BL/6 mice at different days post infection (dpi), and quantitative reverse-transcriptase polymerase chain reaction was performed as described in Materials and Methods. Results are expressed as the logarithm of relative quantity (RQ) calculated from comparative threshold cycle values, as described in Material and Methods. mRNAs values are shown for interferon (IFN)–γ *(A);* tumor necrosis factor (TNF)–α *(B);* interleukin (IL)–4 *(C);* IL-13 *(D);* IL-10 *(E),* transforming growth factor (TGF)–β *(F),* and PGE_2S *(G). Empty bars,* BALB/c mice; *filled bars,* C57BL/6 mice. Results are mean values (±SD) for 3 different mice. All differences observed in infected mice, compared with noninfected mice, were statistically significant, except for *(C)* and *(D)* C57BL/6 mice at 7 dpi and for BALB/c and C57BL/6 mice at all days after infection *(F).* *Significant differences observed between BALB/c and C57BL/6 mice ($P < .05$). A representative experiment (of 3 experiments performed) is shown.

We also analyzed the cellular source of these enzymes. We found that iNOS and arginase II were expressed in the cardiomyocytes of infected BALB/c mice, in agreement with findings from previous reports that attributed a role for arginase II in cardiomyocyte survival [36] and contractility [42]. Interestingly, arginase I expression was detected for the first time in infiltrating $CD68^+$ macrophages only, and, according to protein expression, arginase I was very likely responsible for arginase enzymatic activity in heart tissue. In this regard, previous research reported a role for cruzipain in promoting parasite replication by triggering arginase I expression in macrophages [35]. On the other hand, quantification of $CD68^+$ mRNA in heart tissue showed that the

numbers of these cells were very similar in BALB/c and C57BL/6 mice, indicating that the amount of infiltrating macrophages was not responsible for the increased arginase I expression and activity seen in BALB/c mice. Rather, infiltrating macrophages in infected BALB/c mice expressed more arginase I per cell than did those in C57BL/6 mice.

We found that *T. cruzi* infection triggered iNOS expression in cardiomyocytes, in agreement with previous observations [4]. However, the parasite was unable to induce the expression of arginase I in cardiomyocytes or expression of arginase I and iNOS in resident peritoneal macrophages.

Together, data on in vitro and in vivo infection suggest that induction of iNOS expression in cardiomyocytes could be triggered by the parasite, whereas expression of arginase I in macrophages depends on other factors—very likely, levels of such Th2 cytokines as IL-4 and IL-13, which, in fact, were highly elevated in the heart during infection. Interestingly, we found that cardiomyocytes expressed arginase I at the time of IL-4 stimulation, whereas the parasite alone was unable to induce its expression in vitro. However, arginase I was not observed in the cardiac cells of infected BALB/c mice, even though IL-4 is found in cardiac tissue. Because infection partially inhibits IL-4–induced arginase I in vitro, it is likely that a similar mechanism is operating in vivo.

It is important to note that a discrete induction of arginase I, compared with induction detected in heart tissue, was observed in circulating PBMCs but not in other lymphatic organs of acutely infected mice. In agreement with previous reports [32], this finding indicates that arginase I is preferentially induced in macrophages infiltrating the heart, likely by elevation of the IL-4 and IL-13 levels present in this organ. iNOS protein was not detected in PBMCs but, rather, in heart tissue, suggesting a specific important role of iNOS in this organ.

Our analysis showed that both Th1 and Th2 cytokines were induced at the time of infection in the hearts of both BALB/c and C57BL/6 mice. It is generally accepted that, in response to many parasitic diseases, susceptible BALB/c mice mainly produce Th2 cytokines, whereas resistant C57BL/6 mice mainly produce Th1 cytokines [43]. However, we found that this dichotomy in Th1 and Th2 production is not so strict in *T. cruzi* infection—at least in the heart. Nonetheless, the balance between Th1 and Th2 in the heart is better in C57BL/6 mice than in BALB/c mice, and the levels of Th2 cytokine expression were always higher and persisted longer in susceptible mice than in resistant mice.

The induction of ODC expression could result from the uptake of apoptotic cells during *T. cruzi* infection, which causes release of PGE_2 and induction of TGF-β [44]. Because the ODC substrate depends on arginase, its induction could be mediated by TGF-β. However, very weak induction of TGF-β mRNA was observed, compared with the induction noted for other cytokines, suggesting that TGF-β does not significantly contribute to the induction of arginase I in our model. On the other hand, expression of PGE_2S was significantly higher in BALB/c mice than in C57BL/6 mice at 21 dpi, indicating that PGE_2 could partially contribute to the increased arginase I expression observed in BALB/c mice, compared with C57BL/6 mice.

In the heart, NO has been described to affect cardiac vasodilation and muscle contractility [45]. Our experiments demonstrated that elevated expression of iNOS in the heart tissue during acute *T. cruzi* infection likely generated high levels of NO, which could negatively affect heart function. In contrast, arginase expressed by infiltrated macrophages and cardiomyocytes could control excessive NO production. We found an even higher induction of arginase I after *T. cruzi* infection in the hearts of $iNOS^{-/-}$ mice, which presented less severe myocardial inflammation than did *wt* mice in previous reports [46]. This finding suggests that arginase I could be preventing the development of iNOS-dependent deleterious effects.

During acute *T. cruzi* infection, there is also strong suppression of the T lymphocyte responses mediated by myeloid cells expressing NO [5]. In addition, L-arginine depletion could cause inhibition of T cell activation by decreasing CD3ζ expression [47]. Because arginase is a marker of myeloid suppressor cells (MSCs) involved in immune suppression [48], it is possible that the induction of iNOS and arginase seen in infected hearts suppresses T cell activation in the heart, allowing parasite replication. In this direction, it is tempting to speculate that arginase-expressing infiltrated macrophages are either M2 macrophages or MSCs, although further characterization needs to be done.

In summary, we analyzed arginine metabolism enzymes in the heart and showed, for the first time, that arginase I is expressed by infiltrated macrophages during acute experimental *T. cruzi* infection. This finding suggests that arginase I could have a role in the regulation of the immune response in heart tissue and in the development of cardiac pathology. Questions as to whether arginase I may play a role in host cell and parasite growth, counteracting NO-dependent vasodilation and cardiac muscle contractility, will be addressed in the future. However, our immediate research will focus on characterization of heart-infiltrated macrophages and elucidation of the role of IL-4 and IL-13 in the induction of arginase in heart tissue during acute infection in mice.

Acknowledgments

S.G. and M.P.A. are researchers with Consejo Nacional de Investigaciones Científicas y Técnicas de Argentina (CONICET). We thank Isabel Chico-Calero and Hugo Salgado for the animal care and Maria A. Chorro and Carlos Chillón for their technical assistance.

References

1. Vincendeau P, Gobert AP, Daulouède S, Moynet D, Mossalayi MD. Arginases in parasitic diseases. Trends Parasitol **2003**; 19:9–12.
2. Aliberti JC, Machado FS, Souto JT, et al. β-Chemokines enhance parasite uptake and promote nitric oxide-dependent microbiostatic activity in murine inflammatory macrophages infected with *Trypanosoma cruzi.* Infect Immun **1999**; 67:4819–26.

3. Munoz-Fernández MA, Fernández MA, Fresno M. Activation of human macrophages for the killing of intracellular *Trypanosoma cruzi* by TNF-α and IFN-γ through a nitric oxide-dependent mechanism. Immunol Lett **1992**; 33:35–40.
4. Machado FS, Martins GA, Aliberti JC, Mestriner FL, Cunha FQ, Silva JS. *Trypanosoma cruzi*-infected cardiomyocytes produce chemokines and cytokines that trigger potent nitric oxide-dependent trypanocidal activity. Circulation **2000**; 102:3003–8.
5. Goni O, Alcaide P, Fresno M. Immunosuppression during acute *Trypanosoma cruzi* infection: involvement of Ly6G ($Gr1^+$)$CD11b^+$ immature myeloid suppressor cells. Int Immunol **2002**; 14:1125–34.
6. Noël W, Raes G, Hassanzadeh Ghassabeh G, De Baetselier P, Beschin A. Alternatively activated macrophages during parasite infections. Trends Parasitol **2004**; 20:126–33.
7. Corraliza IM, Soler G, Eichmann K, Modolell M. Arginase induction by suppressors of nitric oxide synthesis (IL-4, IL-10 and PGE_2) in murine bone-marrow-derived macrophages. Biochem Biophys Res Commun **1995**; 206:667–73.
8. Pegg AE. Regulation of ornithine decarboxylase. J Biol Chem **2006**; 281: 14529–32.
9. Munder M, Eichmann K, Modolell M. Alternative metabolic states in murine macrophages reflected by the nitric oxide synthase/arginase balance: competitive regulation by $CD4^+$ T cells correlates with Th1/Th2 phenotype. J Immunol **1998**; 160:5347–54.
10. Boutard V, Havouis R, Fouqueray B, Philippe C, Moulinoux JP, Baud L. Transforming growth factor-β stimulates arginase activity in macrophages: implications for the regulation of macrophage cytotoxicity. J Immunol **1995**; 155:2077–84.
11. Morris SM Jr, Kepka-Lenhart D, Chen LC. Differential regulation of arginases and inducible nitric oxide synthase in murine macrophage cells. Am J Physiol **1998**; 275:E740–7.
12. Daghigh F, Fukuto JM, Ash DE. Inhibition of rat liver arginase by an intermediate in NO biosynthesis, N^G-hydroxy-L-arginine: implications for the regulation of nitric oxide biosynthesis by arginase. Biochem Biophys Res Commun **1994**; 202:174–80.
13. Mössner J, Hammermann R, Racké K. Concomitant down-regulation of L-arginine transport and nitric oxide (NO) synthesis in rat alveolar macrophages by the polyamine spermine. Pulm Pharmacol Ther **2001**; 14: 297–305.
14. Sonoki T, Nagasaki A, Gotoh T, et al. Coinduction of nitric-oxide synthase and arginase I in cultured rat peritoneal macrophages and rat tissues in vivo by lipopolysaccharide. J Biol Chem **1997**; 272: 3689–93.
15. El-Gayar S, Thüring-Nahler H, Pfeilschifter J, Röllinghoff M, Bogdan C. Translational control of inducible nitric oxide synthase by IL-13 and arginine availability in inflammatory macrophages. J Immunol **2003**; 171:4561–8.
16. Lee J, Ryu H, Ferrante RJ, Morris SM Jr, Ratan RR. Translational control of inducible nitric oxide synthase expression by arginine can explain the arginine paradox. Proc Natl Acad Sci USA **2003**; 100:4843–8.
17. Wanasen N, MacLeod CL, Ellies LG, Soong L. L-arginine and cationic amino acid transporter 2B regulate growth and survival of *Leishmania amazonensis* amastigotes in macrophages. Infect Immun **2007**; 75:2802–10.
18. Yeramian A, Martin L, Serrat N, et al. Arginine transport via cationic amino acid transporter 2 plays a critical regulatory role in classical or alternative activation of macrophages. J Immunol **2006**; 176:5918–24.
19. Gobert AP, Cheng Y, Wang JY, et al. *Helicobacter pylori* induces macrophage apoptosis by activation of arginase II. J Immunol **2002**; 168:4692–700.
20. Gobert AP, McGee DJ, Akhtar M, et al. *Helicobacter pylori* arginase inhibits nitric oxide production by eukaryotic cells: a strategy for bacterial survival. Proc Natl Acad Sci USA **2001**; 98:13844–9.
21. Huang J, DeGraves FJ, Lenz SD, et al. The quantity of nitric oxide released by macrophages regulates *Chlamydia*-induced disease. Proc Natl Acad Sci USA **2002**; 99:3914–9.
22. Gobert AP, Daulouede S, Lepoivre M, et al. L-arginine availability modulates local nitric oxide production and parasite killing in experimental trypanosomiasis. Infect Immun **2000**; 68:4653–7.
23. Noël W, Hassanzadeh G, Raes G, et al. Infection stage-dependent modulation of macrophage activation in *Trypanosoma congolense*-resistant and -susceptible mice. Infect Immun **2002**; 70:6180–7.
24. Iniesta V, Gómez-Nieto LC, Corraliza I. The inhibition of arginase by N^{ω}-hydroxy-L-arginine controls the growth of *Leishmania* inside macrophages. J Exp Med **2001**; 193:777–84.
25. Iniesta V, Gómez-Nieto LC, Molano I, et al. Arginase I induction in macrophages, triggered by Th2-type cytokines, supports the growth of intracellular *Leishmania* parasites. Parasite Immunol **2002**; 24:113–8.
26. Iniesta V, Carcelén J, Molano I, et al. Arginase I induction during *Leishmania major* infection mediates the development of disease. Infect Immun **2005**; 73:6085–90.
27. Kropf P, Fuentes JM, Fähnrich E, et al. Arginase and polyamine synthesis are key factors in the regulation of experimental leishmaniasis in vivo. FASEB J **2005**; 19:1000–2.
28. Bergeron M, Olivier M. *Trypanosoma cruzi*-mediated IFN-γ-inducible nitric oxide output in macrophages is regulated by iNOS mRNA stability. J Immunol **2006**; 177:6271–80.
29. Gazzinelli RT, Oswald IP, Hieny S, James SL, Sher A. The microbicidal activity of interferon-γ-treated macrophages against *Trypanosoma cruzi* involves an L-arginine-dependent, nitrogen oxide-mediated mechanism inhibitable by interleukin-10 and transforming growth factor-β. Eur J Immunol **1992**; 22:2501–6.
30. Metz G, Carlier Y, Vray B. *Trypanosoma cruzi* upregulates nitric oxide release by IFN-γ-preactivated macrophages, limiting cell infection independently of the respiratory burst. Parasite Immunol **1993**; 15:693–9.
31. Pakianathan DR, Kuhn RE. *Trypanosoma cruzi* affects nitric oxide production by murine peritoneal macrophages. J Parasitol **1994**; 80: 432–7.
32. Fabrino DL, Leon LL, Parreira GG, Genestra M, Almeida PE, Melo RC. Peripheral blood monocytes show morphological pattern of activation and decreased nitric oxide production during acute Chagas' disease in rats. Nitric Oxide **2004**; 11:166–74.
33. Giordanengo L, Guiñazu N, Stempin C, Fretes R, Cerbán F, Gea S. Cruzipain, a major *Trypanosoma cruzi* antigen, conditions the host immune response in favor of parasite. Eur J Immunol **2002**; 32: 1003–11.
34. Stempin C, Giordanengo L, Gea S, Cerbán F. Alternative activation and increase of *Trypanosoma cruzi* survival in murine macrophages stimulated by cruzipain, a parasite antigen. J Leukoc Biol **2002**; 72: 727–34.
35. Stempin CC, Tanos TB, Coso OA, Cerbán FM. Arginase induction promotes *Trypanosoma cruzi* intracellular replication in Cruzipain-treated J774 cells through the activation of multiple signaling pathways. Eur J Immunol **2004**; 34:200–9.
36. Aoki MP, Guiñazú NL, Pellegrini AV, Gotoh T, Masih DT, Gea S. Cruzipain, a major *Trypanosoma cruzi* antigen, promotes arginase-2 expression and survival of neonatal mouse cardiomyocytes. Am J Physiol Cell Physiol **2004**; 286:C206–12.
37. European Convention. Council directive from the Convention for the Protection of Vertebrate Animals Used for Experimental and Other Scientific Purposes (Strasbourg, France). 18 March 1986.
38. Piron M, Fisa R, Casamitjana NL, et al. Development of a real-time PCR assay for *Trypanosoma cruzi* detection in blood samples. Acta Trop **2007**; 103:195–200.

39. Corraliza IM, Campo ML, Soler G, Modolell M. Determination of arginase activity in macrophages: a micromethod. J Immunol Methods **1994**; 174:231–5.
40. Wang GW, Schuschke DA, Kang YJ. Metallothionein-overexpressing neonatal mouse cardiomyocytes are resistant to H_2O_2 toxicity. Am J Physiol **1999**; 276:H167–75.
41. Cummings KL, Tarleton RL. Inducible nitric oxide synthase is not essential for control of *Trypanosoma cruzi* infection in mice. Infect Immun **2004**; 72:4081–9.
42. Steppan J, Ryoo S, Schuleri KH, et al. Arginase modulates myocardial contractility by a nitric oxide synthase 1-dependent mechanism. Proc Natl Acad Sci USA **2006**; 103:4759–64.
43. Fresno M, Kopf M, Rivas L. Cytokines and infectious diseases. Immunol Today **1997**; 18:56–8.
44. Freire-de-Lima CG, Nascimento DO, Soares MB, et al. Uptake of apoptotic cells drives the growth of a pathogenic trypanosome in macrophages. Nature **2000**; 403:199–203.
45. Barouch LA, Harrison RW, Skaf MW, et al. Nitric oxide regulates the heart by spatial confinement of nitric oxide synthase isoforms. Nature **2002**; 416:337–9.
46. Chandra M, Tanowitz HB, Petkova SB, et al. Significance of inducible nitric oxide synthase in acute myocarditis caused by *Trypanosoma cruzi* (Tulahuen strain). Int J Parasitol **2002**; 32:897–905.
47. Rodriguez PC, Zea AH, DeSalvo J, et al. L-arginine consumption by macrophages modulates the expression of CD3ζ chain in T lymphocytes. J Immunol **2003**; 171:1232–9.
48. Bronte V, Serafini P, Apolloni E, Zanovello P. Tumor-induced immune dysfunctions caused by myeloid suppressor cells. J Immunother (1997) **2001**; 24:431–46.